Radiative corrections to the pressure and the one-loop polarization tensor of massless modes in SU (2) Yang-Mills thermodynamics

Markus Schwarzy, Ralf Hofmanny, and Francesco Giacosa

^yInstitut fur Theoretische Physik Universitat Heidelberg Philosophenweg 16 69120 Heidelberg, Germany

Institut fur Theoretische Physik

Johann Wolfgang Goethe { Universitat

Max von Laue { Str. 1

D-60438 Frankfurt am Main, Germany

A bstract

We compute the one-loop polarization tensor—for the on-shell, massless mode in a thermalized SU (2) Yang-Mills theory being in its deconning phase. Postulating that SU (2)_{CMB} today July, we discuss 'se ect on the low-momentum part of the black-body spectrum at temperatures 2 c.4 Twhere T_{CMB} 2:7 K. A table-top experiment is proposed to test the above postulate. As an application, we point out a possible connection with the stability of dilute, cold, and old innergalactic atom ic hydrogen clouds. We also compute the two-loop correction to the pressure arising from the instantaneous massless mode in unitary-C oulomb gauge, which formerly was neglected, and present in proved estimates for subdominant corrections.

1 Introduction

In [1] a nonperturbative approach to SU (2) and SU (3) Yang-M ills them odynam ics was put forward. Here we are only concerned with the decon ning phase for the case SU (2).

Brie y speaking, the idea on how to attack strongly interacting, thermalized SU (2) gauge dynamics in an analytical way is as follows: At high temperatures T a ground state is generated out of interacting calorons and anticalorons. Since, on the microscopic level, there is no analytical access to this highly complex dynamical situation an average over all space involving a noninteracting caloron-anticaloron system of trivial holonomy [2] is performed to derive the phase $\frac{1}{1-1}$ of a macroscopic adjoint scalar eld . Subsequently, the existence of a Yang-Mills scale By xing the modulus j j and T together determ ine how large a nite spatial volum e needs to be to saturate the above in nite-volum e average. Next, one observes that the eld neither uctuates quantum mechanically nor statistically. To com plete the analysis of the ground-state dynam ics the Yang-M ills equations for the (coarse-grained) gauge elds in the topologically trivial sector is solved subject to a source term provided by : A pure-gauge solution exists which shifts the vanishing energy density and pressure due to the noninteracting, BPS saturated caloron and 4 ³T. M icroscopically, the negative anticaloron to nite values, Pgs = gs = ground state pressure is due to the (anti)caloron's holonomy shift by gluon exchange generating a constituent m onopole and antim onopole [4, 5, 6, 7, 8] subject to a mutual force induced by quantum uctuations 9]. Notice that attraction is much more likely than repulsion [1] explaining the negative ground-state pressure that emerges after spatial coarse-graining. It is stressed that the potential V () is unique: the usual shift am biquity V()! V()+ const, which occurs due to the second-order nature of the Euler-Lagrange equations when applied to a given e ective theory, is absent since the solution to these equation needs to be BPS saturated and periodic in the Euclidean time [1, 10].

A first an adm issible rotation to unitary gauge, each of the two o -C artan modes is seen to acquire a mass m = 2ej jwhile the Cartan mode remains massless. Here e denotes the elective gauge coupling after coarse-graining. As in [1] we will refer to o -C artan modes as tree-level heavy (TLH) and to Cartan modes as tree-level massless (TLM). Demanding the invariance of Legendre transformations between them odynamical quantities when going from the fundamental to the elective theory, a rst-order evolution equation for e = e(T) follows. There exists an attractor to the evolution. Namely, the behavior of e(T) at low temperatures is independent of the initial value. The plateau, e = 5:1, expresses the constancy of magnetic charge attributed to an isolated, screened monopole which is liberated by a dissociating, large-holonomy caloron [1, 9]. At $T_{cE} = 11:65 - 1$ the function elever diverges

¹A part from the term describing the interaction with the action for the topologically trivial sector after spatial coarse-graining looks the same as the fundamental Yang-Mills action. The ultimate reason for this is the perturbative renormalizability of Yang-Mills theory [3].

as e(T) $log(T T_E)$. Thus for $T T_{C,E}$ a total screening of the isolated magnetic charge of a monopole takes place. This implies the latter's masslessness, its condensation and the decoupling of the TLH modes.

O m itting in unitary-C oulom b gauge the 'propagation' of the 0-com ponent of the TLM mode ($A_0^{a=3}$), it was shown in [11] that the two-loop correction is negative and and that the ratio of its modulus to the free quasiparticle pressure is at most 10^3 . It peaks at T $3T_{c,E}$. Neglecting $hA_0^3(x)A_0^3(y)$ i was justified by the observation that the real part of the electric screening mass $\lim_{p \to 0} \frac{1}{100} = 0$; p) diverges. Here denotes the one-loop polarization tensor of the TLM mode [1]. In the present work we investigate in detail how reliable such an approximation is.

The paper is organized as follows: In Sec. 2 we present the elective theory, list its Feynm an rules in the physical gauge (unitary-Coulomb), and discuss the constraints on loop-momenta emerging from the spatial coarse-graining. A calculation of the polarization tensor for an on-shell TLM mode (associated with the photon when postulating that SU (2)_{CMB} $\stackrel{\text{today}}{=}$ U (1)_Y [1, 12, 13]) is perform ed in Sec.3. We discuss the em ergence of a gap in the low-frequency dom ain of the black-body spectrum at $_{\text{CM}}$ $_{\text{B}}4$ Where T_{CM} $_{\text{B}}$ 2:7 K . A table-top experim ent is proposed tem peratures accordingly. Moreover, we aim at an explanation for the stability of cold, dilute, old, and large atom ic hydrogen clouds recently observed within our galaxy. In Sec. 4 we present improved estimates for subdominant two-bop pressure corrections. Next we re-calculate exactly the dom inant correction involving the nonlocal diagram: the propagation' of the 0-com ponent of the TLM mode is now taken in to account. On a qualitative level, our present results con m those obtained in [1]. In the last section a sum mary and outlook on future research are presented.

2 P rerequisites

Let us give a brief introduction into the e ective theory for them alized SU (2) Y ang-M ills dynam ics being in its decon ning phase [1]. The following e ective action emerges upon spatial coarse-graining down to a length scale equal to j j 1 = $\frac{2}{3}$:

$$S = \text{tr}$$
 d d^3x $\frac{1}{2}G$ G $+$ D D $+$ d^{-6} : (1)

In Eq.(1) G $G^a = (A^a + A^a) + (A^a + A^b) + (A^b) + (A^b)$

$$a = 2 e^{3=2}$$
 (2)

 $^{^2}$ At $T_{c;E}$ the ground state becomes instable with respect to the formation of a large caloron holonomy [9].

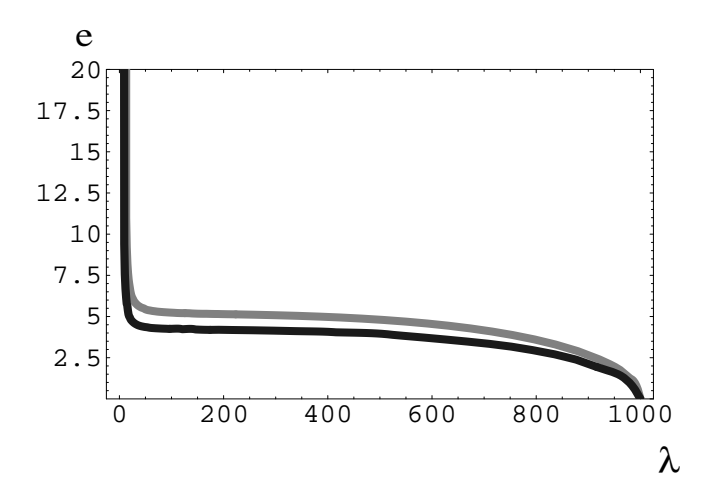


Figure 1: The one-loop evolution of the excitive gauge coupling e=e() for SU (2) (grey curve) and SU (3) (black curve). The choice of the initial condition a ($_{\rm P}=1000$) = 0 is arbitrary, the low-tem perature behavior is una exted by changing $_{\rm P}$ as long as $_{\rm P}$ is considerably larger than $_{\rm CE}$ [1].

from the (inverted) solution of the (one-loop) evolution equation

$$\theta_{a} = \frac{24^{-4}a}{2^{-6}}D$$
 (2a)

w here

 $\frac{2}{T}$, and a $\frac{m}{T}$. The (coarse-grained) caloron-anticaloron ensemble is integrated into the non-uctuating adjoint scalar eld 11, 10]. Eq.(3) guarantees the invariance of the Legendre transform ations between therm odynamical quantities when going from the fundamental to the excitive theory. Notice that in deriving Eq.(3) the vacuum part in the one-loop expression for the pressure P can safely be neglected [1]. In Figs.1 and 2 the one-loop evolution of e and that of $\frac{P}{T^4}$, $\frac{P}{T^4}$ are depicted.

Our calculations are performed within the real-time formulation of nite-temperature eld theory [4]. Let us formulate the Feynman rules: The free propagator

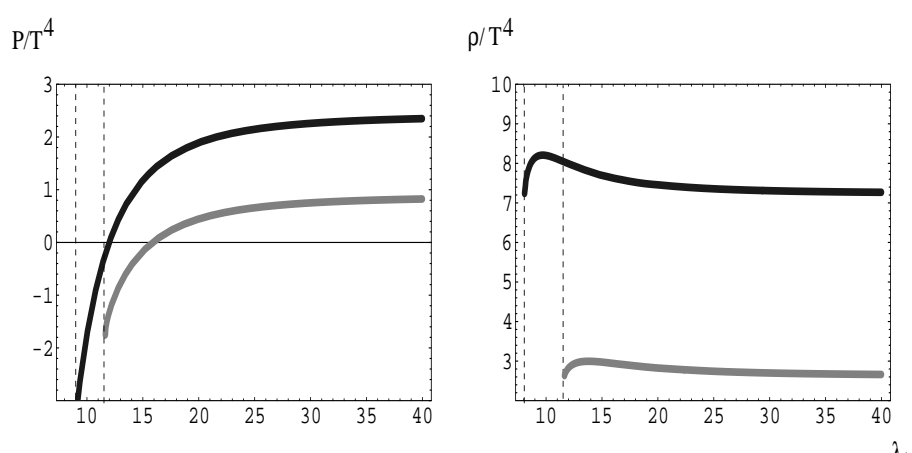


Figure 2: Ratio of the free quasiparticle pressure P and T⁴ (left panel) and the free quasiparticle energy density and T⁴ (right panel) for SU (2) and SU (3) (grey and black, respectively) as a function of $\frac{2}{2}$ [1].

 $D^{TLH;0}$ of a TLH mode in unitary-Coulomb gauge³ is

$$D_{jab}^{TLH;0}(p) = abD^{c} \frac{i}{p^{2} m^{2}} + 2 (p^{2} m^{2})n_{B}(\dot{p}_{0}) = T)$$
 (5)

$$D^{\circ} = g \frac{p p}{p^2} \tag{6}$$

where n_B (x) = 1=(e^x 1) denotes the Bose-E instein distribution function. For the free TLM mode we have

$$D_{ab;}^{TLM;0}(p) = ab P^{T} \frac{i}{p^{2}} + 2 (p^{2})n_{B}(\dot{p}_{0}) = T) \frac{u u}{p^{2}} : (7)$$

w here

$$P_{T}^{00} = P_{T}^{0i} = P_{T}^{i0} = 0$$
 (8)

$$P_{T}^{ij} = ^{ij} p^{j} = p^{2} :$$
 (9)

TLM modes carry a color index 3 while TLH modes have a color index 1 and 2. Notice the term / u u in Eq.(7) describing the 'propagation' of the A_0^3 eld. Here u = (1;0;0;0) represents the four-velocity of the heat bath.

 $^{^3}$ This is a completely xed, physical gauge in the elective theory after spatial coarse-graining: First one rotates and a pure-gauge ground-state eld a^{bg} to = $_3$ j j and $a^{bg}=0$. This is an admissible gauge rotation which, however, changes the value of the Polyakov loop P from 1 to 1. Up to a nite renormalization this result coincides with the full expectation hP i because there are massless TLM modes in the spectrum [1]. Subsequently, one xes the remaining U (1) gauge freedom by imposing $\theta_i A_i^3 = 0$. This gauge can always be reached with a periodic gauge function such that exp[i]2U(1): (=0;x)=(=:x).

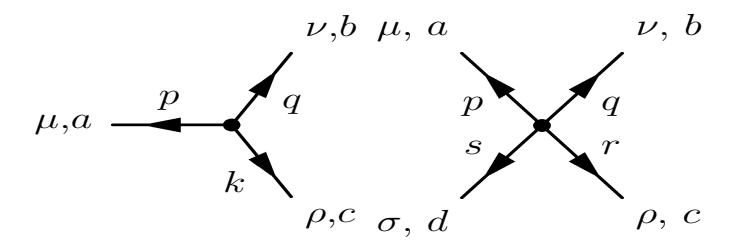


Figure 3: Three- and four-vertices.

The three- and four-gauge-boson vertices are given as

$$g_{abc}(p;k;q) = e(2)^4 (p+q+k)f_{abc}(g(q p)+g(k q)+g(p k)]$$

(10)

with the fourm omenta and color indices de ned in Fig3. A coording to [14] one has to divide a loop-diagram by i and by the number of its vertices.

The analytical description of the nontrivial ground-state dynam ics is facilitated by a spatial coarse-graining down to a resolution j j. Thus the maximalo -shellness of gauge modes is $constrained^4$ to be [1]

$$\dot{\mathbf{p}}^2 \quad \mathsf{m}^2 \,\dot{\mathsf{j}} \quad \dot{\mathsf{j}} \,\, \dot{\mathsf{j}} \,\, \tag{12}$$

where m = 0 for a TLM mode and m = 2e j j= 2e $\frac{3}{2 \text{ T}}$ for a TLH mode. Moreover, the resolution associated with a four vertex of ingoing momenta p; k is constrained as

$$j(p + k)^2 j \quad j \stackrel{?}{2}$$
: (13)

Notice that the constraint in (13) is only applicable if two of the four legs associated with the vertex form a closed loop. If this is not the case then one needs to distinguish s, t, and u-channel scattering.

 $^{^4}$ The idea of a W ilsonian renormalization-group ow is realized after the interacting topologically nontrivial sector has been integrated out. At each loop order (expansion in h 1) a modication of the on-shell condition emerges which determines the restriction on admissible o-shellness for the next loop order.

3 One-loop polarization tensor for an on-shell TLM mode

3.1 General considerations

Here we compute the diagonal components of the polarization tensor $(p_0;p)$ for the TLM mode at the one-loop level specializing to $p^2=0$. This is conceptually interesting and provides for a prediction associated with a modi cation of the low-momentum part of black body spectra at low temperatures. Moreover, a computation of $^{ii}(p_0;p)$ is necessary for an analytical grasp of the physics related to the large-angle regime in CMB maps.

For any value of p^2 the polarization tensor for the TLM mode is transversal,

$$p = 0: (14)$$

Hence the following decomposition holds

$$= G (p_0; p) P_{T} + F (p_0; p) P_{T}$$
 (15)

w here

$$P_{L} = \frac{p p}{p^2} \quad g \quad P_{T} : \tag{16}$$

The functions $G(p_0;p)$ and $F(p_0;p)$ determine the propagation of the interacting TLM mode. For = 0 Eq.(15) yields upon rotation to real-time

$$F(p_0;p) = 1 + \frac{p_0^2}{p^2}$$
 00: (17)

Assuming p to be parallel to the z-axis, we have

$$_{11} = _{22} = G (p_0; p) :$$
 (18)

In the Euclidean formulation the interacting propagator D $_{ab}^{TLM}$ (p) reads

$$D_{ab;}^{TLM}(p) = \int_{ab}^{n} P^{T} \frac{1}{G p^{2}} + \frac{p^{2}}{p^{2}} \frac{1}{F p^{2}} u u^{O}$$
(19)

Notice that for F=G=0 and rotating to M inkowskian signature Eq.(19) transforms into Eq.(7). In [1] ⁰⁰ was calculated for $p_0=0$ and in the lim it p!=0.0 ne has $j^{00}(0;p!=0)j=f(0;p!=0)j=1$. A coording to Eq.(19) the term / u u vanishes in this lim it. One of the tasks of the present paper is to check how reliable it is to neglect this term altogether when calculating the two-loop corrections to the pressure.

Going on-shell, $\dot{p}_0\dot{j}!$ $\dot{p}\dot{j}$ in Eq.(17), we observe that F! 0 provided that remains nite in this lim it. We have computed 00 for $p^2=0$ and we have seen

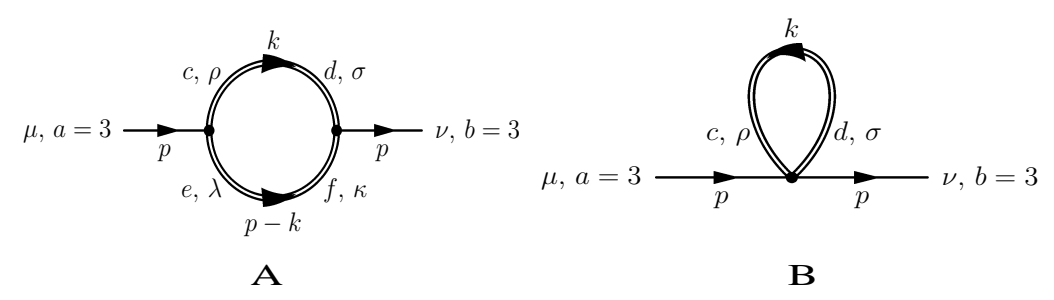


Figure 4: The diagram s for the TLM mode polarization tensor.

that this is, indeed, the case. This, in turn, implies that the longitudinal structure (quantum 'propagation') in Eq.(19) reduces to the free limit as in Eq.(7). The function G modi es the dispersion law for the TLM mode as follows:

$$!^{2}(p) = p^{2} + ReG(!(p);p);$$

 $(p) = \frac{1}{2!} Im G(!(p);p):$ (20)

For technical sim plicity we evaluate $_{11} = G$ for $p_0 = pj$. A ssum ing that G(!(p);p) is analytic about !=pj and that it depends only weakly on !, an interpretation of this result in the sense of Eq. (20) is facilitated. Namely, setting !=pj the right-hand side of Eq. (20) represents a useful approximation to the exact solution $!^2(p)$ which is expanded in powers of !pj. Notice that the constraint in !(2) does not allow for a large deviation from !=pj anyhow.

3.2 Calculation of G

is the sum of the two diagrams A and B in Fig.4. For $p^2 = 0$ diagram A vanishes. This can be seen as follows. We have

$$A (p) = \frac{1}{2i} \frac{d^4k}{(2)^4} e^2 \cos [g (p k) + g (k p + k) + g (p k + p)]$$

$$dbf [g (k p) + g (p + p k) + g (p + k + k)]$$

$$(cd) g \frac{k k}{k^2} \frac{i}{k^2 m^2} + 2 (k^2 m^2) n_B (k_0 + p)$$

$$(ef) g \frac{(p k) (p k)}{(p k)^2}$$

$$\frac{i}{(p k)^2 m^2} + 2 (k^2 m^2) n_B (k_0 + p)$$

$$\frac{i}{(p k)^2 m^2} + 2 (k_0 k_0 + p)$$

$$\frac{(p k) (p k)}{(p k)^2}$$

(21)

From the one-loop evolution [1] we know that e 5:1. Due to constraint (12) the vacuum part in the TLH propagator thus is forbidden. Using $p^2=0$ and $k^2=m^2$, the therm alpart $_{A,\text{therm}}$ (p) reads

$${}^{A,\text{them}}(p) = ie^{2} \frac{d^{4}k}{(2)^{2}} {}^{h} 2kp {}^{4} \frac{(kp)^{2}}{m^{2}} g + 12 \frac{kp}{m^{2}} k k + 6 + \frac{kp}{m^{2}} (k p + k p) + 5 + \frac{(kp)^{2}}{m^{4}} p p$$

$$(k^{2} m^{2}) n_{B} (k_{0} \neq T) (k_{D} k_{0}^{2} m^{2}) n_{B} (p_{0} k_{0} \neq T) :$$
(22)

For $p_0 > 0$ the product of -functions can be rewritten as

$$(p^{2} k) m^{2}) = \frac{1}{4p_{0} k j k j k^{2} + m^{2}}$$

$$h p \frac{1}{k^{2} + m^{2}} cos \frac{p \frac{1}{k^{2} + m^{2}}!}{k j} + \frac{1}{k^{2} + m^{2}}!$$

$$k_{0} p \frac{1}{k^{2} + m^{2}} cos + \frac{p \frac{1}{k^{2} + m^{2}}!}{k^{2} + m^{2}}!$$

$$k_{0} + p \frac{1}{k^{2} + m^{2}} cos + \frac{p \frac{1}{k^{2} + m^{2}}!}{k^{2} + m^{2}}!$$

$$(23)$$

where g(p;k). Because $\frac{p}{\frac{k \cdot f + m^2}{k \cdot j}} > 1$ and g(p;k). Because $\frac{p}{\frac{k \cdot f + m^2}{k \cdot j}} > 1$ and g(p;k). The argument of the two functions in Eq. (23) never vanishes and thus the right-hand of Eq. (22) is zero. Applying the Feynman rules of Sec. 2, diagram B reads

$$(p) = \frac{1}{i} \frac{Z}{(2)^4} (ab) g \frac{k k}{k^2} \frac{i}{k^2 m^2} + 2 (k^2 m^2) n_B (jk_0 j = T)$$

$$(ie^2) [abe cde (g g g g g) + ace bde (g g g g g) + ace bde (g g g g g)] ;$$

$$(24)$$

Again, the part in Eq. (24) arising from the vacuum contribution in Eq. (5) vanishes because of constraint (12). Applying constraint (13) for $p_0 > 0$; $p^2 = 0$ yields:

$$j(p + k)^{2}j = j2pk + k^{2}j = 2p_{0}(k_{0} + jkjcos) + 4e^{j}f$$

$$= 2p_{0} + k^{2} + 4e^{2}jf + jkjcos + 4e^{2}jf + jf$$
(25)

For the + sign the condition in Eq.(25) is never satis ed, for the sign there is a range for p_0 where the condition is not violated.

We are interested in $\frac{11}{T^2} = \frac{22}{T^2} = \frac{G}{T^2}$ as a function of $X = \frac{\dot{p}\,\dot{p}}{T}$ and $\frac{2\,T}{T}$ when p is parallel to the z-axis. Perform ing the k_0 -integration in Eq. (24) and introducing dim ensionless variables as

$$y = \frac{k}{j j}; \tag{26}$$

we obtain from Eq. (24) that

$$\frac{G}{T^{2}} = \frac{11}{T^{2}} = \frac{22}{T^{2}} = \frac{2}{T^{2}} = \frac{e^{2}}{3} \quad Z = \frac{Z}{3} + \frac{Y_{1}^{2}}{4e^{2}} = \frac{n_{B}}{2} \quad Z = \frac{3}{2} + \frac{y_{1}^{2}}{y^{2} + 4e^{2}}$$
(27)

where the integration is subject to the following constraint:

1
$$^{3=2}\frac{X}{}$$
 $^{p}\frac{y^{2}+4e^{2}}{y^{2}+4e^{2}}+y_{3}+4e^{2}$ 1: (28)

In view of constraint (28) the integral in Eq. (27) is evaluated most conveniently in cylindrical coordinates,

$$y_1 = \cos'; \quad y_2 = \sin'; \quad y_3 = :$$
 (29)

Let us now discuss how the constraint (28) is implemented in the -and -integration. Constraint (28) is re-cast as

$$\frac{4e^2}{3=2}\frac{1}{X} \qquad p \frac{1}{2+2+4e^2} + \frac{4e^2+1}{3=2}\frac{1}{X} : \tag{30}$$

Notice that Eq.(30) gives an upper bound for : $<\frac{4e^2+1}{3-2}\frac{1}{x}$. In contrast, there is no such global lower bound for .

The upper \lim its for the -and -integration are obtained as follows. Since < we can square the second part of the inequality (30) and solve for :

$$\frac{1}{X} = \frac{(4e^2 + 1)^2}{3} = \frac{2}{X} = \frac{4e^2 + 1}{3=2} = 4\hat{e} \qquad M (X;;) : (31)$$

The condition that the expression under the square root in Eq.(31) is positive yields the upper lim it $_{\rm M}$ (X;) for the —integration:

$$\frac{1}{2X} \frac{4e^2 + 1}{3=2} \quad 2^{\frac{X}{4}} \quad 3=2 \frac{e^2}{4e^2 + 1} \quad M \quad (X;) : \tag{32}$$

The lower limit for the —integration is obtained as follows. Upon subtracting from the set part of the inequality 30) the result can be squared provided that $<\frac{4e^2}{3=2}\frac{1}{x}$. Solving for , we have

$$\frac{1}{X} = \frac{(4e^2 - 1)^2}{3} = \frac{2}{X} = \frac{4e^2 - 1}{3=2} = 4e^2 = \frac{1}{m} (X; ;) :$$
 (33)

The condition that the expression under the square root in Eq. (33) is positive introduces the critical value $_{\rm m}$ (X;) for the $_{\rm m}$ integration as:

$$_{m}$$
 (X;) $\frac{4e^{2}}{2x} \frac{1}{3=2} 2^{\frac{X}{3}=2} \frac{e^{2}}{4e^{2}}$: (34)

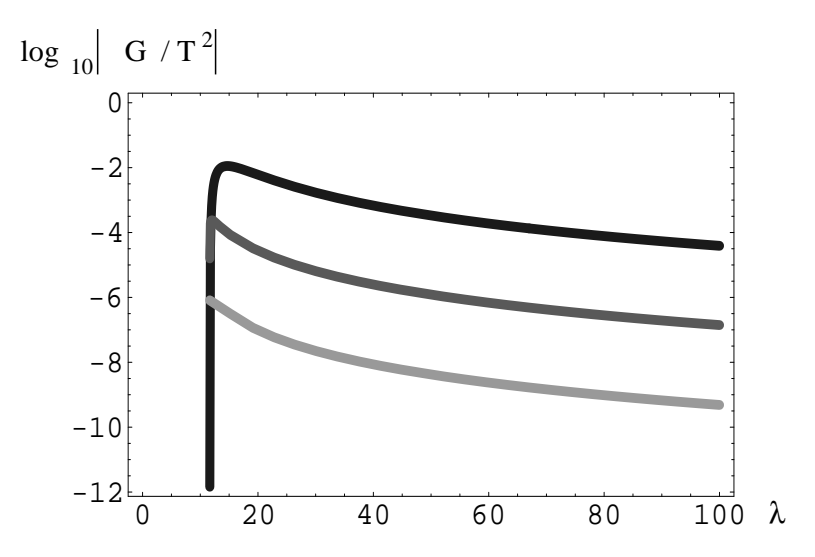


Figure 5: $\frac{G}{T^2}$ as a function of $\frac{2 T}{T}$ for X = 1 (black), X = 5 (dark grey), and X = 10 (light grey).

For 1 < $_{\rm m}$ (X;) the lower limit for the -integration is given by $_{\rm m}$ (x; ;). Notice that according to Eq.(34) $_{\rm m}$ (X;) is always smaller than $\frac{4{\rm e}^2}{3-2}\frac{1}{{\rm x}}$ such that our above assumption is consistent. A coording to Eq.(30), the opposite case, $\frac{4{\rm e}^2}{3-2}$ $_{\rm m}$ (X;), leads to 0 which does not represent an additional constraint. To sum marize, we have

$$\frac{G}{T^{2}} = \begin{array}{c} \text{"Z}_{\text{m}}(x;) & \text{Z}_{\text{M}}(x;;) & \text{Z}_{\text{M}}$$

where the integral operation indicated in the square brackets is applied to the last line.

3.3 Results and discussion

3.3.1 General discussion of results

In Figs.5 and 6 we show plots of $\log_{10} \frac{G}{T^2}$ as obtained by a numerical integration. We have used the one-loop evolution of the elective coupling e=e(). For all and values of X to the right of the dips in Fig.6 $\frac{G}{T^2}$ is negative and real (antiscreening). A coording to the dispersion law in Eq. (20) this implies that the energy of a propagating TLM mode is reduced as compared to the free case. For X values to the left of the dips $\frac{G}{T^2}$ is positive and real (screening) with interesting consequences for the low-momentum regime of black-body spectra, see Sec.3.3.2. Fig.5 indicates the dependence of $\log_{10} \frac{G}{T^2}$ on keeping X=1;5;10 xed. Obviously, the election the propagation of TLM modes arising from TLH intermediate states is very small (maximum of $\frac{G}{T^2}$ at X=1: 10^2). As for the high-temperature behavior we observe the following. On the one hand, there is clear evidence for a power-like suppression of $\frac{G}{T^2}$ in . Recall that the one-loop result for the (quasiparticle) pressure

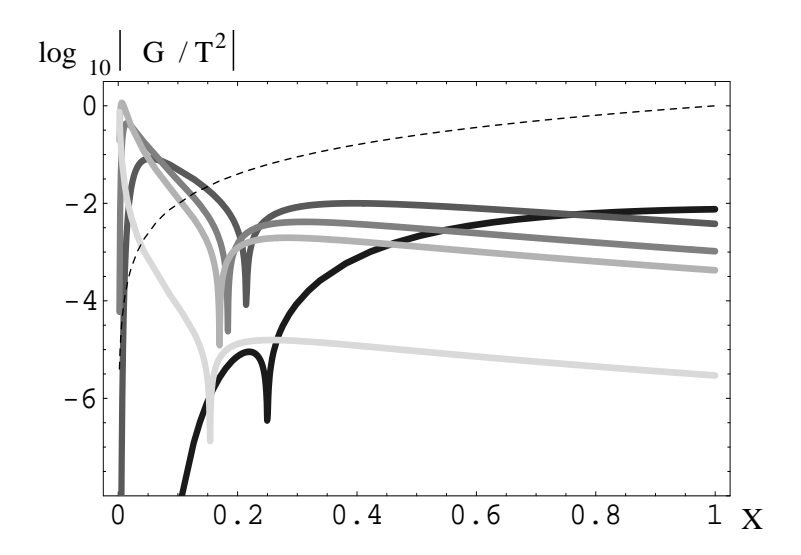


Figure 6: $\frac{G}{T^2}$ as a function of X $\frac{j \cdot j}{T}$ for = 13 (black), = 2 $_{\text{c,E}}$ (dark grey), = 3 $_{\text{c,E}}$ (grey), = 4 $_{\text{c,E}}$ (light grey), = 20 $_{\text{c,E}}$ (very light grey). The dashed curve is a plot of the function f (X) = $2\log_{10} X$. TLM m odes are strongly screened at X -values for which $\log_{10} \frac{G}{T^2} > f$ (X) ($\frac{G}{T} > X$), that is, to the left of the dashed line.

shows a power-like approach to the Stefan-Boltzm ann lim it [1]. In a sim ilar way, the approach to the lim it of vanishing antiscreening is also power-like for the TLM mode. On the one hand, a sudden drop of $\frac{G}{T^2}$ occurs for & $_{\rm C,E}=11.65$. This signals that intermediary TLH modes decouple due to their diverging mass. On the other hand, the values of $\log_{10} \frac{G}{T^2}$ at xed > $_{\rm C,E}$ are equidistant for (nearly) equidistant values of X . This shows the exponential suppression of $\log_{10} \frac{G}{T^2}$ for X 1 and can be understood as follows. For large X Eq. (30) demands to be negative and j j to be large. As a consequence, the square root in Eq. (30), which appears as an argument of $n_{\rm B}$, see Eq. (35), is large thus implying exponential suppression in X .

Fig.6 indicates the dependence of $\log_{10} \frac{G}{T^2}$ on X keeping = 13, = 2 $_{\text{c;E}}$, $3_{c,E}$, $4_{c,E}$, and $= 20_{c,E}$ xed. Notice that the rst value for $_{\text{C.E.}} = 11.65$ and that the low-m omentum regime is investigated. Namely, for X 1 the afore-mentioned exponential suppression sets in which can be seen by the linear decrease. For X < 0.8 the black curve (= 13) is below the curves for = $2_{c;E}$; $3_{c;E}$; $4_{c;E}$ because of the vicinity of to $6_{c;E}$ where the mass of TLH m odes diverges. The sm allness of the curve for $= 20_{\rm c.f.}$ arises due to the abovediscussed power suppression. Notice the sharp dip occurring for X-values in the 03. The dip is caused by a change in sign for G: For X to the range 0:15 Χ right of the dip G is negative (antiscreening) while it is positive (screening) to the left. The dashed line is a plot of the function $f(X) = 2 \log_{10} X$. The intersection of a curve with f(X) indicates the momentum where the dynamical mass of the TLM mode is equal to the modulus of its spatial momentum (strong screening), see Eq.(20). For c:E or for c:E the strong-screening regime shrinks to the

point X=0. While $\frac{G}{T^2}$ is practically zero in the former case it is sizable in the latter. For $=2_{c,E}$; $4_{c,E}$ Fig. 6 shows that the strong-screening regime has a nite support beginning at $X_s=0.15$. The fact that within our approximation $p^2=0$ no imaginary part is being generated in $\frac{G}{T^2}$ is related to the vanishing of diagram A, see Eq. (21). For $p^2 \notin 0$ diagram A is purely imaginary and thus would lead to an additional damping in propagating modes. Since we are interested in TLM modes $p^2=0$ we expect the elect of diagram A to be negligible.

3.3.2 Application to SU $(2)_{CMB}$

In [1,12] the postulate was put forward that the photon (regarded as a propagating wave) is identified with the TLM mode of an SU (2) Yang-Mills theory with scale $10^4\,\mathrm{eV}:$ SU (2)_{CMB}. For the present cosmological epoch we have T_{C;E} = T_{CMB} 2:7 K $10^4\,\mathrm{eV}$. The viability of such a postulate was discussed and checked in view of cosmological and astrophysical bounds in [13].

As discussed in Sec.3.3.1 today's photon, which propagates above the ground state of SU (2)_{CMB}, is una ected by nonabelian uctuations (TLH modes) because of the decoupling of the latter. For radiation of a temperature considerably above T_{CMB} , for example room temperature ($\frac{1}{40}\,\text{eV}$), a detection of the distortion of the black-body spectrum at low momenta surely is outside the reach of experiments, see Fig.6. This is, however, no longer true if the temperature is a few times T_{CMB} .

W e thus propose the following table-top experiment for an independent check of the above postulate: The wave-length $l_{\rm s}$ of the strongly screened mode (X < X $_{\rm s}$ = 0.14T) at T = $2\,T_{\rm CMB}$ (about the boiling temperature of liquid $^4{\rm H}$ e) is given as

$$l_s = \frac{h c}{k_B T X_s} = 1.9 cm$$
 (36)

To detect the absence of low-m omentum modes (X $_{\rm S}=0.14\,\rm T$) in the black-body spectrum at T = $2\,T_{\rm CMB}$, at least one linear dimension d of the isolated cavity should be considerably larger than $1.9\,\rm cm$, say d $50\,\rm cm$.

In [15] the construction of a low-tem perature black body (LTBB), to be used as a tem perature norm al, was reported for tem perature ranges 80 K $\,$ T $\,$ 300 K . For the lower lim it T = 80 K we obtain X $_{\rm S}$ = 0.0285 corresponding to $l_{\rm S}$ = 0.63 cm .

Let us now discuss how sensitive the measurement of the LTBB spectral intensity I (X) needs to be in order to detect the spectral gap setting in at X $_{\rm s}$. A useful criterion is determined by the ratio R (X $_{\rm s}$) of I (X $_{\rm s}$) and I (X $_{\rm max}$) where X $_{\rm max}$ = 2:82 is the position of the maximum of I (X) (back to natural units):

$$R(X_s) = \frac{I(X_s)}{I(X_{max})} = \frac{1}{1.42144} \frac{X_s^3}{\exp(X_s)} = 1:$$
 (37)

For $T=80\,\text{K}$ we have $R(X_s=0.0285)=5$ 10^4 . To achieve such a high precision is a challenging task. To the best of the authors know ledge in [15] only the overall and not the spectral intensity of the LTBB was measured. For $T=5\,\text{K}$ one has

R (X $_{\rm S}=0:14)=1:3$ 10^2 . Thus at very low tem peratures the precision required to detect the spectral gap is within the 1% -range. It is, however, experimentally challenging to cool the LTBB down to these low tem peratures. To the best of the authors know ledge a precision measurement of the low-frequency regime of a LTBB at T=5 T=0 LTBB at T=5 LTBB

3.3.3 Possible explanation of the stability of innergalactic clouds of atom ic hydrogen at T 5 10K

In [16, 17] the existence of a large (up to $2\,\mathrm{kpc}$), old (estim ated age 50 m illion years), cold (m ean brightness tem perature T_B 20 K with cold regions of T_B 5 10 K), dilute (number density: 1.5) cand m assive (1.9 10 solarm asses) innergalactic cloud (G SH 139-03-69) of atom ic hydrogen (H I) forming an arc-like structure in between spiralarm swas reported. In [18] and references therein smaller structures of this type were identified. These are puzzling results which do not the dominant model for the interstellar medium [17]. Moreover, considering the typical time scale for the formation of H_2 out of H I of about $10^6\,\mathrm{yr}$ [18] at these low temperatures and low densities clashes with the inferred age of the structure observed in [16].

To the best of the authors know ledge there is no standard explanation for the existence and the stability of such structures. We wish to propose a scenario possibly explaining the stability based on SU(2)_{CMB}. Namely, at temperatures $T_B = 5 = 10\,\mathrm{K}$, corresponding to $T_B = 0.15\,T_B > \dot{p}_{cj} > \dot{p}_{low}$ j is such that it forbids their propagation (strong screening), see Figs. 6 and 7, where \dot{p}_{low} j depends rather strongly on temperature (Fig.7).

Incidentally, the regime for the wavelength l_c associated with p_c j is comparable to the interatom ic distance 1 cm in G SH I39-03-69: At T = 5K we have l_c = 1.95 cm l_c 19:87 cm = l_c , at T = 10K we have l_c = 1:31 cm l_c 2:06 m = l_c . Thus the (almost on-shell) photons being emitted by a given HI particle to mediate the dipole interaction towards another HI particle are far of their mass shell at typical interatom ic distances. As a consequence, the dipole force at these distances appears to be switched of the H2 molecules are prevented from forming at these temperatures and densities.

At this point we would like to discuss an apparent paradox involving the concept of a spin tem perature T_S for G SH I39-03-69. The latter is de ned as a tem perature associated with the 21 cm -line em itted and absorbed by spin- ips within the H I system. For this line to propagate, a ne-tuning of the brightness tem perature T_B of the cloud would be needed, see Fig.7, because photons that are absent at wavelengths 1 cm would be required at the wavelength 21 cm to maintain the thermal equilibrium in the spin system. The question whether or not thermal equilibrium is

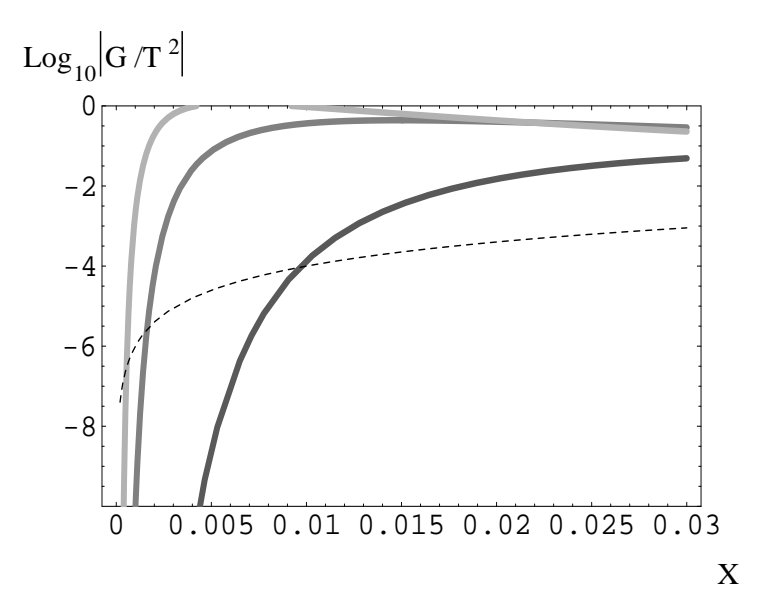


Figure 7: $\frac{G}{T^2}$ as a function of X $\frac{\dot{p}\,\dot{j}}{T}$ for =2 $_{\text{c,E}}$ (dark grey), =3 $_{\text{c,E}}$ (grey), and =4 $_{\text{c,E}}$ (light grey) and very low momenta. The dashed curve is a plot of the function f (X) = $2\log_{10} X$. TLM modes are strongly screened for X > X $_{\text{low}}$ for which $\log_{10}\frac{G}{T^2}$ > f (X).

realized in the latter is, however, not directly accessible to observation: W hile $T_{\rm B}$ is directly observable by a determ ination of the distance of non-illum inated cloud regions and the em itted intensity of the 21 cm -line the determ ination of $T_{\rm S}$ hinges on assumptions on the optical depth and various other brightness temperatures [18].

The astrophysical origin of the structure G SH I39-03-69 appears to be a mystery. The point we are able to make here is that once such a cloud of H I particles has formed it likely remains in this state for a long period of time.

4 Two-loop corrections to the pressure revisited

4.1 General considerations

In [11] the two loop corrections to the pressure of an SU (2) Yang-M ills theory in its decon ning phase were calculated om itting the term / u u in Eq. (7). Here we take this term into account in our calculation. The two-loop corrections to the

Figure 8: Two-loop corrections to the pressure.

pressure are calculated as indicated in Fig.8.0 ne has

$$P = P_{\text{nonlocal}} + P_{\text{local}} :$$
 (38)

The analytical expressions take the form

$$P_{local} = \frac{1}{8i} \frac{Z}{(2)^4} \frac{d^4k}{(2)^4} \frac{d^4p}{(2)^4} _{[4]abcd} D _{;ab}(k) D _{;cd}(p)$$
 (39)

and

$$P_{\text{nonlocal}} = \frac{1}{8i} \frac{Z}{(2)^4} \frac{d^4k}{(2)^4} \frac{d^4p}{(2)^4} _{\text{[B]abc}}(p;k; p k)_{\text{[B]rst}}(p; k;p+k)$$

$$D_{\text{par}}(p)D_{\text{pb}}(k)D_{\text{pct}}(p k):$$
(40)

D ;ab stands for the appropriate TLH and TLM propagator. The calculation proceeds along the lines of [11]: Because of the constraint (12) and the fact that e 5:1 as a result of the one-loop evolution [1] the vacuum parts in the TLH propagators do not contribute. A firer sum m ing over color indices and contracting Lorentz indices the -functions associated with the thermal parts of the TLH propagators render the integration over the zero components of the loop momenta trivial. The remaining integrations of spatial momenta are performed in spherical coordinates. At this point both constraints (12) and (13) are used to determine the boundary conditions for these integrations.

4.2 Localdiagram s

Let us rst introduce a useful convention: Due to the split of propagators into vacuum and therm alcontributions in Eqs. (5) and (7) combinations of therm aland vacuum contributions of TLH and TLM propagators arise in Eqs. (39) and (40). We will consider these contributions separately and denote them by

$$P_{x}^{X}YZ$$
 and $P_{x}^{X}Y$ (41)

for the nonlocal diagram and the local diagram s in Fig.8, respectively. In Eq.(41) capital rom an letters take the values H or M, indicating the propagator type (TLH/TLM), and the associated small greek letters take the values v (vacuum) or t (therm al) or c (Coulomb, the term / u u in Eq.(7)).

The correction P_{tt}^{HH} was computed exactly in [11]. (The contributions P_{vt}^{HH} and P_{vv}^{HH} vanish due to (12).) The correction om itted in [11] is P_{tc}^{HM} :

$$P_{tc}^{HM} = \frac{e^{2}}{8} \frac{Z}{(2)^{4}} \frac{d^{4}k}{(2)^{4}} \frac{d^{4}p}{(2)^{4}}$$

$$f_{ac} f_{db} (g g g g g) + f_{ad} f_{bc} (g g g g g) = \frac{p p}{p^{2}} 2 (p^{2} m^{2}) n_{B} (\dot{p}_{0} \dot{j} - T) \frac{iu u}{k^{2}} :$$
(42)

Sum ming over color indices and contracting the Lorentz indices, see Fig.9, yields

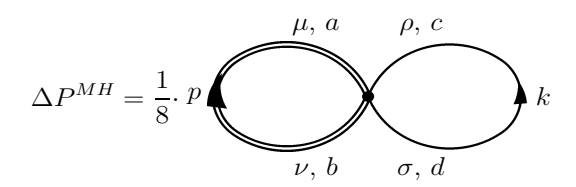


Figure 9: The diagram for P^{HM} .

$$P_{tc}^{HM} = \frac{e^2}{2}^{\frac{Z}{2}} \frac{d^4k}{(2)^4} \frac{d^4p}{(2)^4} + 2 + \frac{(p_0)^2}{p^2} + 2 + (p^2 - m^2) n_B (p_0 = T) \frac{i}{k^2}; \quad (43)$$

Notice that P_{tc}^{HM} is manifestly imaginary indicating that it must be canceled by the imaginary part of P_{tv}^{HM} (The nonlocal diagram is manifestly real.). We are only able to estimate the modulus j P_{tc}^{HM} j. This is done in the following.

Integrating over p_0 and introducing dimensionless variables as x $p \neq j \neq j y$ $k \neq j j$ and z cos cos cos (p;k), we have

$$P_{tc}^{HM} = \frac{ie^{2} + 2X}{2(2)^{5}} X X Z dx dy dz d 3 + \frac{x^{2}}{4e^{2}} \frac{x^{2} n_{B} (2 - 3e^{2})^{2} \overline{x^{2} + 4e^{2}})}{x^{2} + 4e^{2}} (44)$$

where $\frac{p}{p^2 + m^2}$. In dimensionless variables the constraints (12) and (13) read

$$\mathbf{\dot{j}}^2$$
j $\mathbf{\dot{j}}^2$ **j** ! 1 $\mathbf{\dot{i}}^2$ $\mathbf{\dot{p}}$ 1 $\mathbf{\dot{p}}$ 1 (45) $\mathbf{\dot{j}}$ $\mathbf{\dot{p}}$ + $\mathbf{\dot{k}}$) $\mathbf{\dot{j}}$! 1 $\mathbf{\dot{4}e}$ 2 $\mathbf{\dot{z}}$ 2xyz+ $\mathbf{\dot{z}}$ 2xyz+ $\mathbf{\dot{z}}$ 2 1: (46)

On the one hand, to implement both conditions (45) and (46) exactly is technically very involved. On the other hand, neglecting condition (46), as was done for P_{tv}^{HM} in [11], turns out to be insulcient for the correction P_{tc}^{HM} . Therefore, we fully consider (45) and partly in plement (46) in our calculation.

The integrand of Eq. (44) is positive de nite. Condition (46) represents a bound on a positive-curvature parabola in . Considering only the minimum $_{m \text{ in}}(x) = \frac{a \text{ positive-curvature parabola, relaxes the restrictions on } x$, y, and z meaning that the integration of the positive de nite integrand is over a larger area than (46) actually permits. Thus we obtain an upper bound for P_{tc}^{HM} . Replacing with $_{m \text{ in}}$, condition (46) reads

1
$$\hat{x} + y^2 + 2xyz$$
 h(x;y;z) 1: (47)

Because this result is obtained for both signs of p_0 ! $p^2 + m^2$ we have p_0 = 2. Let us now investigate the behavior of the function p_0 have p_0 to the that p_0 have p_0 investigate the behavior of the function p_0 have p_0 have p_0 investigate the behavior of the function p_0 have p_0 have

1 because $h(x;y; 1) = (x \ \dot{y})$ 0. The upper bound h(x;y;z) 1 puts restrictions on the upper $\lim_{x \to 0} \lim_{x \to 0} h(x;y;z)$ for the z-integration where

$$z_{+} (x; y) = \frac{1 - x^{2} - y^{2}}{2x y}$$
: (48)

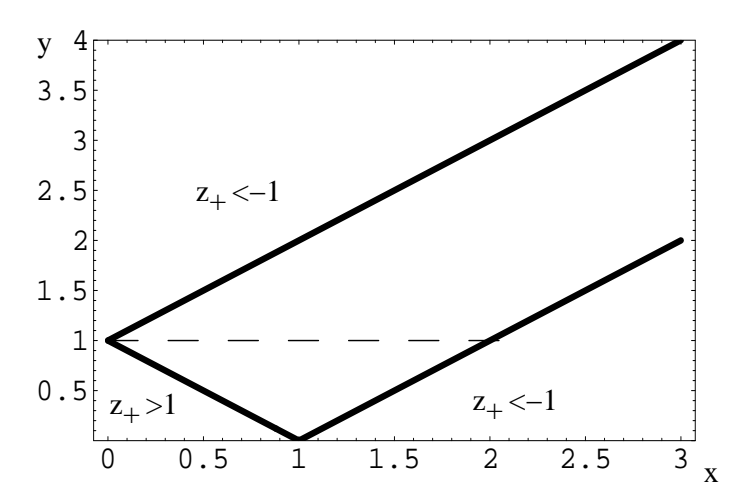


Figure 10: A dm issible range for the x-and y-integration. The regions with $z_+ < 1$ are forbidden, the dashed line represents the function y = 1.

Hence z runs within the range 1 z m in (1;z(x;y)). The next task is to determ ine the range for x and y for which 1 z(x;y) 1. Setting z(x;y) > 1, we have

0
$$y < y(x)$$
 $x + 1$: (49)

Setting z_+ (x;y) > 1, we have

0
$$y(x)$$
 x 1 < y < $y(x)$ x + 1: (50)

The adm issible range for x and y is depicted in Fig. 10.

To obtain \lim its on the -integration we solve condition (45) for . For y 1 we have

$$p = \frac{p}{y^2 - 1}$$
 $p = \frac{p}{y^2 + 1}$ or $p = \frac{p}{y^2 + 1}$ $p = \frac{p}{y^2 - 1}$: (51)

For 0 y < 1 we have
$$p \frac{1}{y^2 + 1}$$
 $p \frac{1}{y^2 + 1}$ (52)

Finally, we obtain:

$$P_{tc}^{HM} \leftarrow SSGM1.$$

$$h^{Z}_{1} \quad Z_{y} \quad Z_{1} \quad Z_{y}^{P}_{\overline{y^{2}+1}} \quad Z_{1} \quad Z_{1} \quad Z_{z}, \quad Z_{y}^{P}_{\overline{y^{2}+1}}$$

$$\leq \quad dx \quad dy \quad dz \quad p_{\overline{y^{2}+1}} \quad d \quad dx \quad dy \quad dz \quad p_{\overline{y^{2}+1}} \quad d \quad +$$

$$\quad Z_{2} \quad Z_{1} \quad Z_{z}, \quad Z_{y}^{P}_{\overline{y^{2}+1}} \quad Z_{2} \quad Z_{y}, \quad Z_{z}, \quad Z_{y}^{P}_{\overline{y^{2}+1}}$$

$$\quad dx \quad dy \quad dz \quad p_{\overline{y^{2}+1}} \quad d \quad + 2 \quad dx \quad dy \quad dz \quad p_{\overline{y^{2}+1}} \quad d \quad +$$

$$\quad Z_{1} \quad Z_{y}, \quad Z_{z}, \quad Z_{y}^{P}_{\overline{y^{2}+1}} \quad i$$

$$\quad Z_{1} \quad Z_{y}, \quad Z_{z}, \quad Z_{y}^{P}_{\overline{y^{2}+1}} \quad i$$

$$\quad Z_{1} \quad Z_{y}, \quad Z_{z}, \quad Z_{z}^{P}_{\overline{y^{2}+1}} \quad i$$

$$\quad Z_{1} \quad Z_{y}, \quad Z_{z}, \quad Z_{z}^{P}_{\overline{y^{2}+1}} \quad i$$

$$\quad Z_{1} \quad Z_{y}, \quad Z_{z}, \quad Z_{z}^{P}_{\overline{y^{2}+1}} \quad i$$

$$\quad Z_{1} \quad Z_{y}, \quad Z_{z}, \quad Z_{z}^{P}_{\overline{y^{2}+1}} \quad i$$

$$\quad Z_{1} \quad Z_{y}, \quad Z_{z}, \quad Z_{z}^{P}_{\overline{y^{2}+1}} \quad i$$

$$\quad Z_{1} \quad Z_{y}, \quad Z_{z}, \quad Z_{z}^{P}_{\overline{y^{2}+1}} \quad i$$

$$\quad Z_{1} \quad Z_{y}, \quad Z_{z}, \quad Z_{z}^{P}_{\overline{y^{2}+1}} \quad i$$

$$\quad Z_{1} \quad Z_{y}, \quad Z_{z}, \quad Z_{z}^{P}_{\overline{y^{2}+1}} \quad i$$

$$\quad Z_{1} \quad Z_{y}, \quad Z_{z}, \quad Z_{z}^{P}_{\overline{y^{2}+1}} \quad i$$

$$\quad Z_{1} \quad Z_{y}, \quad Z_{z}^{P}_{z}, \quad Z_{z}^{P}_$$

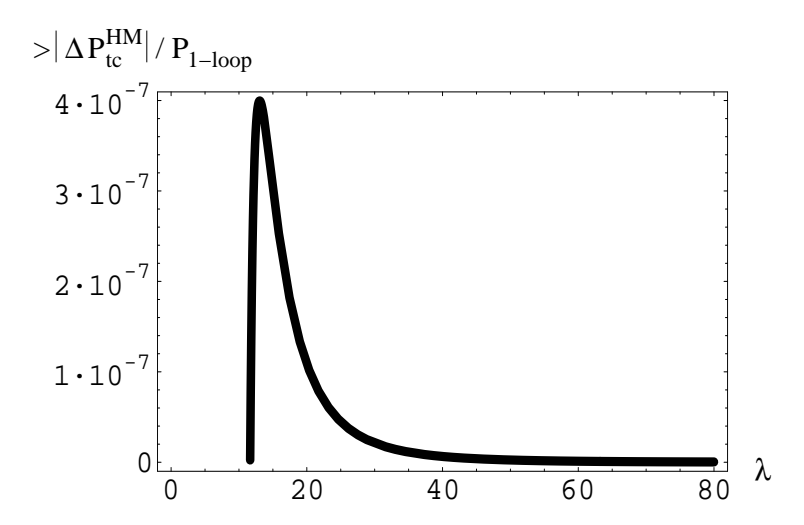


Figure 11: Upper estimate for the modulus $P_{tc}^{HM} = P_{1-loop}$ as a function of where P_{1-loop} is the pressure due to one-loop uctuations. (The ground-state part in P is omitted in P_{1-loop} [1].)

In Fig.11 a plot of the estimate for $P_{tc}^{\,\mathrm{H}\,\mathrm{M}}$ is shown as a function of .

The next object to be considered is $P_{tv}^{H\,M}$. We know that $P_{tc}^{H\,M}$ is purely imaginary and thus is canceled by the imaginary part of $P_{tv}^{H\,M}$. Therefore the interesting quantity is Re $P_{tv}^{H\,M}$. We will be content with an upper estimate for Re $P_{tv}^{H\,M}$. This signicantly improves the estimate for j $P_{tv}^{H\,M}$ jas it was obtained in [11] by a Euclidean rotation and by subsequently implementing the constraint (12) only. Here we would like to obtain a tighter estimate by also implementing (13) strictly along the lines developed for $P_{tv}^{H\,M}$. We have

$$P_{tv}^{HM} = \frac{e^{2}}{2} \frac{Z}{(2)^{4}} \frac{d^{4}k}{(2)^{4}} \frac{d^{3}p}{(2)^{3}} dp_{0} n_{B} \quad P_{\overline{p^{2} + m^{2}} = T} \frac{i}{k^{2} + i}$$

$$4 + \frac{p^{2}}{m^{2}} \frac{(pk)^{2}}{m^{2}k^{2}} \frac{p_{0} \quad P_{\overline{p^{2} + m^{2}}} + p_{0} + P_{\overline{p^{2} + m^{2}}}}{2^{p} \overline{p^{2} + m^{2}}} :$$
(54)

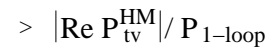
Going over to dimensionless variables, in our treatment of condition (46) both choices for the sign of p_0 lead to one and the same constraint (47). Therefore the integral over the sum of -functions in Eq. (64) yields a factor of two. Notice that

$$\lim_{! \ 0} Re^{\frac{i}{2} \frac{1}{y^2 + i}} = \lim_{! \ 0} \frac{(^2 y^2)^2 + ^2}{(^2 y^2)^2 + ^2} = (^2 y^2)$$
 (55)

and that the points $^2 = y^2$ are not excluded by (45). Perform ing the integrations over azim uthal angles and , we thus have

Re
$$P_{tv}^{HM}$$

$$\frac{e^{2}}{(2)^{4}} \frac{4}{2^{2}} x^{2} dx dy dz x^{2} y \qquad 4 + \frac{x^{2}}{4e^{2}} \frac{x^{2} z^{2}}{4e^{2}}$$
$$\frac{n_{B} 2}{p} \frac{3 - 2^{p} x^{2} + 4e^{2}}{x^{2} + 4e^{2}}$$
 (56)



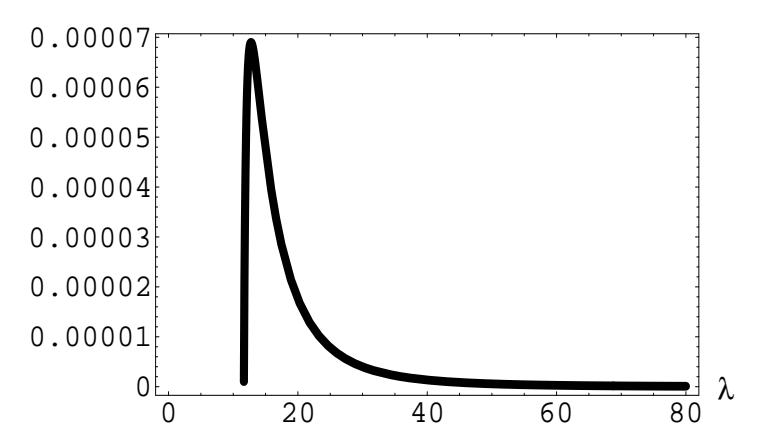


Figure 12: Upper estimate for $\frac{\Re e^{-P \frac{H}{tv}}}{P_{1-loop}}$ as a function of .

Im plem enting constraint (46) in the same way as in our estimate for j P_{tc}^{HM} j yields the result depicted in Fig.12. This estimate is about one order of magnitude better than the one for P_{tv}^{HM} as obtained in [11].

4.3 Nonlocal diagram

Here we compute the correction $P_{ttv}^{H\,H\,M} + P_{ttc}^{H\,H\,M}$. In [11] the correction $P_{ttv}^{H\,H\,M}$ was computed exactly so that we can focus on $P_{ttc}^{H\,H\,M}$. The implementation of (12) is precisely as in [11], only the integrand diers. Summing over color indices, see Fig.13, we have

$$P_{\text{ttc}}^{\text{H H M}} = \frac{e^{2}}{4(2)^{6}} Z d^{4}k d^{4}p d^{4}q (p + k + q) \frac{u u}{q^{2}} i$$

$$g (p q) + g (q k) + g (k p)$$

$$g \frac{p p}{p^{2}} (p^{2} m^{2}) n_{B} \frac{\dot{p}_{0} j}{T} i$$

$$g (p q) + g (q k) + g (k p)$$

$$g \frac{k k}{k^{2}} (k^{2} m^{2}) n_{B} \frac{\dot{p}_{0} j}{T} : (57)$$

Contracting the Lorentz indices is straight forward but cum bersom e. The q-integration is trivial, and the p_0 - and k_0 -integration over the product of delta functions, (p^2 m²), is performed as in [11]. Integrating over azim uthal angles, going over to dimensionless variables, and introducing the abbreviation S (x;e) $x^2 + 4e^2$

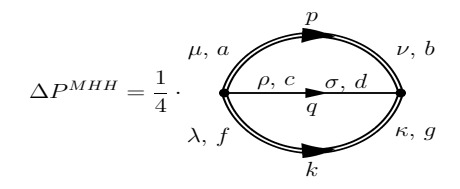


Figure 13: The diagram for P^{HHM} .

yields

$$P_{\text{ttc}}^{\text{H H M}} = \frac{e^{2} + 2}{4(2)^{4}} \frac{Z}{\text{dx dy dz}} \frac{n_{\text{B}} + 2}{x^{2} + y^{2} + 2xyz} \frac{n_{\text{B}} + 2}{x^{2} + y^{2} + 2xyz} \frac{n_{\text{B}} + 2}{x^{2} + y^{2} + 2xyz} \frac{(S(x;e) S(y;e) + xyz)^{2}}{4e^{2}} \frac{(S(x;e) S(y;e) + xyz)^{2}}{4e^{2}} \frac{8e^{2} + x^{2} + y^{2} + 2S(x;e) S(y;e)}{e^{2}} (S(x;e) S(y;e) + xyz) + \frac{8e^{2} + x^{2} + y^{2} + 2S(x;e) S(y;e)}{16e^{4}} (S(x;e) S(y;e) + xyz)^{2} \frac{16e^{4}}{2(8e^{2} + x^{2} + y^{2} + 6S(x;e) S(y;e))} (S(x;e) S(y;e) + xyz)^{2}$$
(58)

As discussed in [11] the z-integration in Eq. (58) is bounded as

1 z max (1; m in (1;
$$z(x; y)$$
)) (59)

w here

$$z_{+}(x;y) = \frac{1}{xy} = \frac{1}{2} + 4e^{2} = S(x;e) S(y;e) :$$
 (60)

The next task is to determ ine the range for x and y for which 1 z(x;y) 1. Provided that x < 10; y < 10 one can solve the condition $z_+(x;y) > 1$ for y. This yields

0 y y(x)
$$\frac{(1+8e^2)x + {}^{p}\overline{1+16e^2}S(x;e)}{8e^2}:$$
 (61)

Notice that the intersection of y(x) with the y-and x-axis is at $y_0 = x_0 = 1 + \frac{1}{16e^2}$ 1. Thus our above assumption certainly is satisfied. Setting z(x;y) > 1, yields

y (x)
$$\frac{(1+8e^{2})x}{8e^{2}} = \frac{p}{1+16e^{2}} S(x;e) = y \qquad y \qquad \frac{(1+8e^{2})x+p}{1+16e^{2}} S(x;e)}{8e^{2}} :$$
(62)

Notice the factor $\frac{1}{x^2+y^2+2xyz}$ in the integrand of Eq. (58). Upon z-integration this transforms into $\log(x^2+y^2+2xyz)\int_1^{\max(-1,\min(1,z_+(x,y)))}$. For z=-1 there is an integrable singularity at x=y presenting a problem for the numerical x- and y-integration. To cope with it we cut out a small band of width 2 centered at x=y

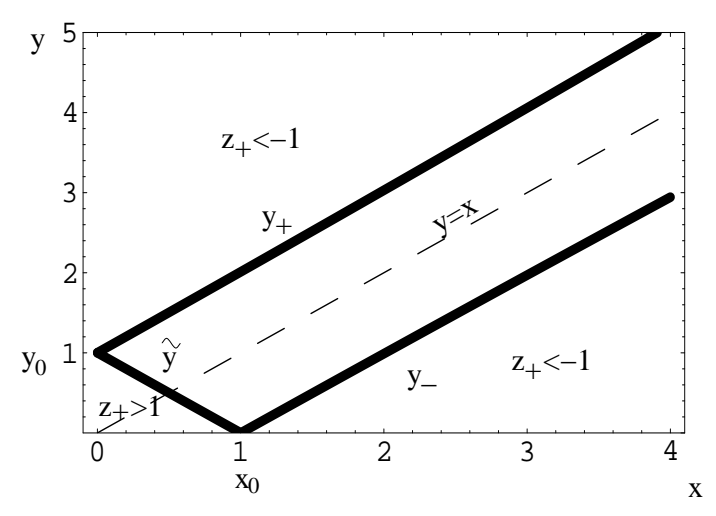


Figure 14: The region of integration in the x y plane corresponding to Eq. 58). $(\Delta P_{ttv}^{HHM} + \Delta P_{ttc}^{HHM})/P_{1-Loop}$

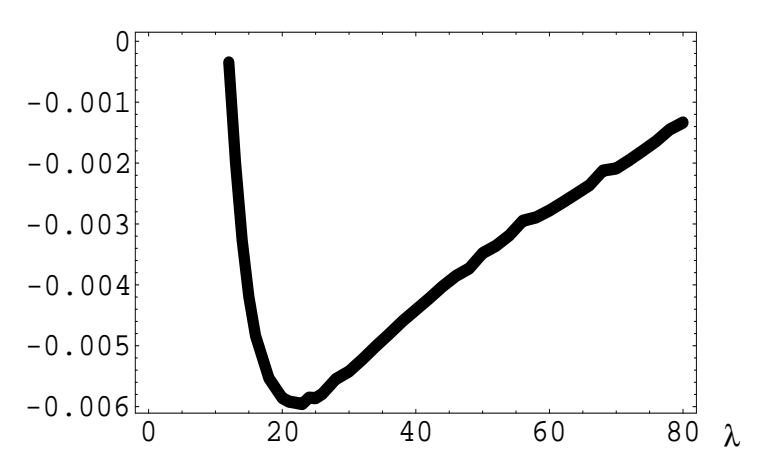


Figure 15: $\frac{P_{ttv}^{HHM} + P_{ttc}^{HHM}}{P_{1-loop}}$ as a function of .

and observe stabilization of the result for ! 0. In Fig.14 the region of integration is depicted in the x-y-plane. The computation of $\frac{P_{\rm th}^{\rm H.H.M.} + P_{\rm th}^{\rm H.H.M.}}{P_{\rm 1-loop}}$ () is performed with a one-loop running coupling e. The result is shown in Fig.15. It is worth mentioning that the result for $\frac{P_{\rm th}^{\rm H.H.M.}}{P_{\rm 1-loop}}$ () in [11] was obtained by using the plateau value e = 5:1 for all . This over-estimates the minimum because it neglects the onset of the logarithmic pole e $\log($ $_{\rm c/E}$). (At this minimum the factor e^2 in front of the integral dominates over the exponential suppression due to $n_{\rm B}$.) Using the running coupling, the minimum is reduced as 1:8 10^3 ! 2:2 10^3 . Including the term $P_{\rm ttc}^{\rm H.H.M.}$, this reduces further to 6 10^3 .

4.4 Sum mary and discussion

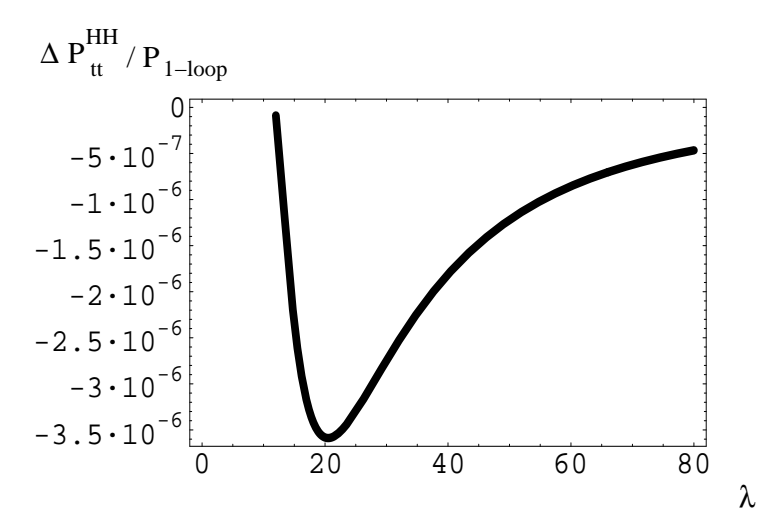
When including the propagation' of the 0-component of the TLM mode in the computation of the two-loop correction to the pressure there are quantitative but not qualitative modications of the results obtained in [1]. This is suggested by the fact that the static electric screening mass diverges [1]. In practice, the diagram that leads to a noticeable modication of the earlier results is the nonlocal one in Fig8. Namely, the correction $\frac{P_{\text{tt}}^{\text{H H M}}}{P_{1-\text{loop}}}$, which was omitted in [11], enhances the modulus of the minimal value of $\frac{P_{\text{tt}}^{\text{H M M}}}{P_{1-\text{loop}}}$ by a factor of about three. Recall that the contribution $\frac{P_{\text{tt}}^{\text{H M}}}{P_{1-\text{loop}}}$ is purely in aginary with a very small modulus and thus is canceled by the in aginary part of $\frac{P_{\text{tt}}^{\text{H M}}}{P_{1-\text{loop}}}$. The modulus of the real part of the latter was estimated in an improved way without invoking a rotation to the Euclidean. As compared to [11] the results for $\frac{P_{\text{tt}}^{\text{H M}}}{P_{1-\text{loop}}}$ and $\frac{P_{\text{tt}}^{\text{H M}}}{P_{1-\text{loop}}}$, as depicted in Figs.16 and 17, are slightly in proved by using the one-loop running coupling and not the plateau value e = 5:1. It is interesting to discuss the (exact) result for the latter in a qualitative way.

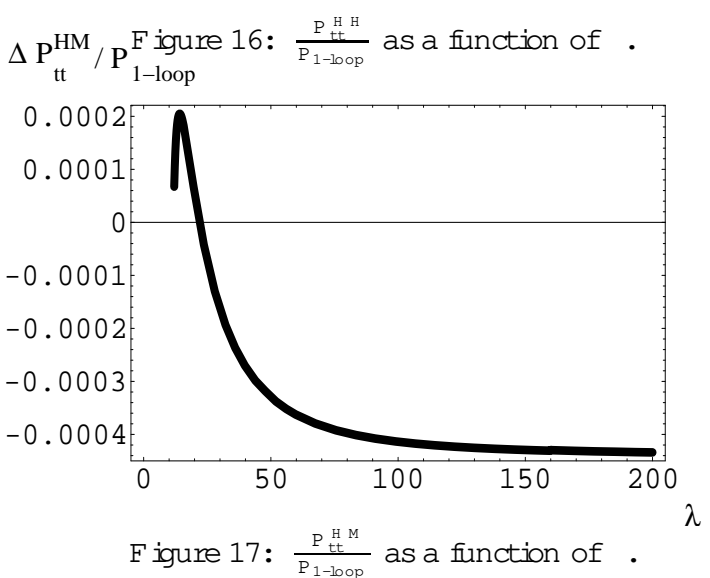
As Fig.17 indicates, the contribution P_{tt}^{HM} is negative and / T^4 since P_{1-loop} / T 4 for large T, see Fig. 2. Let us propose an underlying scenario. First of all this e ect is not due to isolated monopoles (M) and antimonopoles (A) as they are generated by the dissociation of large-holonomy calorons (repulsive M-A potential [9]). (The probability of such processes is suppressed by exp $\frac{m_M + m_A}{T}$ 10 35 [5, 6, 7, 9].) The maximal distance between an M and its A, as generated by sm all-holonomy calorops (attractive M-A potential [9]), is roughly given by the linear dimension j $j^1 = \frac{2 T}{3}$ of the coarse-graining volume. The typical on-shell TLM mode, however, carries a momentum T. Thus for su ciently large T such a mode resolves the magnetic charges of the Morthe Aseparately. If scattering of a TLM mode o of the M or the A within a small-holonomy caloron transfers a m om entum larger than the typical binding energy $E_{\mbox{\tiny bind}}$ of the M -A system then isolated M and A are created. After screening, the masses of the latter are given $\frac{4^{2}}{2}$ T [1]: these particles decouple from the therm odynamics. The TLM mode responsible for this is less energetic after the scattering process, and thus its contribution to the therm odynam ical pressure is dim in ished in comparison to the initial situation. From the observation that P_{tt}^{HM} / T^4 for T $T_{c;E}$ we conclude that the typical E_{bind} / T.

In general, the ground-state part of them odynam ical averages in the deconning phase is perfectly saturated by the physics of small-holonomy calorons. There are, however, observables which are sensitive to the elects of large-holonomy calorons. In particular, such an observable is the spatial string tension $_{\rm S}$, delened as

s
$$\frac{\log \text{ trP exp ig}_{C}^{H} \text{ dl } A_{T}}{S(C)}$$
; (63)

where P is the path-ordering symbol, g denotes the fundam ental coupling, and S (C)





denotes the m in im alarea enclosed by the contour C. The latter should be thought of as being the edge of a square of side-length R in the limit R! 1. From lattice \sin ulations one knows that $_s$ / T^2 at high temperatures. Taking the logarithm of a therm all average, as it is done in Eq. (63), e ectively singles out Boltzmann suppressed contributions. Due to the dissociation of large-holonomy calorons an integration over (nearly) static and screened M and A emerges in the partition function of m icroscopic SU (2) Yang-M ills therm odynam ics [1]. This integration is $\frac{4^{-2}}{2}$ T: The associated subject to a very small Boltzm ann weight due to m $_{\scriptscriptstyle \rm M}$ $m_{\scriptscriptstyle A}$ part of the partition function Z_{M+A} nearly can be factored out. This still holds true for the modi ed partition function when replacing S_{YM} as S_{YM} ! S_{YM} + log trP exp[ig dl A] which is relevant for the evaluation of the average under the logarithm in Eq. (63). It is the M-A factor in the modi ed partition function \mathbb{Z}^0 that generates an area-law (/ R²), additive contribution to the num erator of the right-hand side of Eq. (63) [19]. The rem aining factor in Z^0 describes the dynam ics of uctuating gauge elds and produces a perim eter-law (/ R) contribution. In the \lim it R ! 1 only the M -A contribution survives in the expression for $_{\rm s}$.

5 Sum m ary and outlook

We have computed the one-loop polarization tensor for a massless mode with $p^2=0$ in the decon ning phase of them alized SU (2) Yang-Mills theory. The result indicates that these modes do not propagate (strong screening) in a particular (temperature dependent) low-momentum range at temperatures, say, $2T_{c,E}$

When applying these results to SU (2)_{CMB} [1, 12, 13], identifying the massless mode with our photon, the prediction of a spectral gap in the low-frequency region of the black-body spectrum at T $2\,T_{\text{CMB}}$ $_{\text{CM}}$ 5 2 m erges. Here $T_{\text{CMB}}=2.7\,\text{K}$. An experimental test of this prediction is proposed involving a cavity of linear dimension 50 cm. Such an experiment appears to be well feasible [15].

A nother interesting aspect of our results on the polarization tensor is a possible explanation of the stability of cold, dilute, large, m assive, and old innergalactic clouds of atom ic hydrogen [16, 18, 17]. Namely, the mediation of the dipole interaction between hydrogen atoms, which is responsible for the formation of hydrogen molecules, is switched oat distances on the scale of centimeters. Given the initial situation of an atomic gas of hydrogen with interparticle distance 1 cm and brightness temperature 10 K, as reported in [6], the formation of H $_2$ molecules is extremely suppressed as compared to the standard theory.

In the remainder of the paper we have revisited the computation of the two-loop correction to the pressure rst performed in [1]. On a qualitative level, our improved results agree with those in [11].

Our future activity concerning applications of SU (2) Y ang-M ills therm odynam ics will be focused on the physics of CMB uctuations at low angular resolution.

A cknow ledgem ents

F.G. acknowledges nancial support by the Virtual Institute VH-VI-041 "Dense Hadronic Matter & QCD Phase Transitions" of the Helmholtz Association.

R eferences

- [1] R. Hofm ann, Int. J. Mod. Phys. A 20, 4123 (2005).
- [2] B.J. Harrington and H.K. Shepard, Phys. Rev. D 17, 105007 (1978).
- B] G. 't Hooff, Nucl. Phys. B 33 (1971) 173. G. 't Hooff and M. J. G. Veltman, Nucl. Phys. B 44, 189 (1972). G. 't Hooff, Int. J. Mod. Phys. A 20 (2005) 1336 [arX iv hep-th/0405032].
- [4] W . Nahm, Lect. Notes in Physics. 201, eds. G. Denaro, ea. (1984) p. 189.
- [5] K.-M. Lee and C.-H. Lu, Phys. Rev. D 58, 025011 (1998).

- [6] T.C.K raan and P. van Baal, Nucl. Phys. B 533, 627 (1998).
- [7] T.C.K raan and P. van Baal, Phys. Lett. B 435, 389 (1998).
- [8] R.C.Brower, D.Chen, J.Negele, K.Orginos, and C-ITan, Nucl. Phys. Proc. Suppl. 73, 557 (1999).
- [9] D.Diakonov, N.Gromov, V.Petrov, and S.Slizovskiy, Phys.Rev.D 70,036003 (2004) [hep-th/0404042].
- [10] U.Herbst and R.Hofm ann, hep-th/0411214.
- [11] U. Herbst, R. Hofmann, and J. Rohrer, Acta Phys. Pol. B 36, 881 (2005).
- [12] R. Hofmann, PoS JHW 2005 021 (2006) [hep-ph/0508176].
- [13] F.G iacosa and R.Hofm ann, hep-th/0512184.
- [14] N.P. Landsm an and C.G. van Weert, Phys. Rept. 145, 141 (1987).
- [15] S.P.M orozova et al., M etrologia 30, 369 (1993).
- [16] L.B.G.Knee and C.M.Brunt, Nature 412, 308 (2001).
- [17] J.M.Dickey, Nature 412, 282 (2001).
- [18] D.W. K avars et al., A strophys. J. 626, 887 (2005).
 D.W. K avars and J.M. D ickey et al., A strophys. J. 598, 1048 (2003).
 N.M. M. C. Lure-Gri ths et al., astro-ph/0503134.
- [19] P. Giovannangeli and C. P. Korthals Altes, Talk given at 19th International Symposium on Lattice Field Theory (Lattice 2001), Berlin, Germany, 19-24 Aug 2001, Nucl. Phys. Proc. Suppl. 106, 616 (2002).